A High-Precision Method for In Vitro Proton Irradiation

Michelle E. Howard, PhD[1]*; Janet M. Denbeigh, PhD[1]*; Emily K. Debrot, PhD[2];
Nicholas B. Remmes, PhD[1]; Michael G. Herman, PhD[1]; Chris J. Beltran, PhD[2]

[1]Department of Radiation Oncology, Mayo Clinic, Rochester, MN, USA
[2]University of Wollongong, Wollongong, NSW, Australia
*Michelle E. Howard and Janet M. Denbeigh contributed equally to the work.

Abstract

Purpose: Although proton therapy has become a well-established radiation modality, continued efforts are needed to improve our understanding of the molecular and cellular mechanisms occurring during treatment. Such studies are challenging, requiring many resources. The purpose of this study was to create a phantom that would allow multiple in vitro experiments to be irradiated simultaneously with a spot-scanning proton beam.

Materials and Methods: The setup included a modified patient-couch top coupled with a high-precision robotic arm for positioning. An acrylic phantom was created to hold 4 6-well cell-culture plates at 2 different positions along the Bragg curve in a reproducible manner. The proton treatment plan consisted of 1 large field encompassing all 4 plates with a monoenergetic 76.8-MeV posterior beam. For robust delivery, a mini pyramid filter was used to broaden the Bragg peak (BP) in the depth direction. Both a Markus ionization chamber and EBT3 radiochromic film measurements were used to verify absolute dose.

Results: A treatment plan for the simultaneous irradiation of 2 plates irradiated with high linear energy transfer protons (BP, 7 keV/μm) and 2 plates irradiated with low linear energy transfer protons (entrance, 2.2 keV/μm) was created. Dose uncertainty was larger across the setup for cell plates positioned at the BP because of beam divergence and, subsequently, variable proton-path lengths. Markus chamber measurements resulted in uncertainty values of $\pm$1.8% from the mean dose. Negligible differences were seen in the entrance region ($<$0.3%).

Conclusion: The proposed proton irradiation setup allows 4 plates to be simultaneously irradiated with 2 different portions (entrance and BP) of a 76.8-MeV beam. Dosimetric uncertainties across the setup are within $\pm$1.8% of the mean dose.

Introduction

Proton therapy is a well-established radiation modality for the treatment of various cancers and other diseases. Research has shown an increase in cell-death incidence along the proton Bragg curve (BC), as accounted for in the quantity of relative biologic effectiveness (RBE), ideally, relative to conventional radiotherapy, although a variety of photon radiation types have been used as the reference. The variability of proton RBE is dependent on the change in energy deposition or linear energy transfer (LET) [1–15], among other factors, such as cell type, biologic endpoint, proton energy, and oxygenation [16]. The current RBE value used clinically for proton therapy is 1.1, meaning protons are 10% more effective for all biologic endpoints, including cell death, relative to conventional

Figure 1. Platform setup. (A) Couch with platform holding cell culture plates suspended above the gantry for posterior irradiation. (B) Platform holding cells in reproducible manner at 2 positions along the Bragg curve.
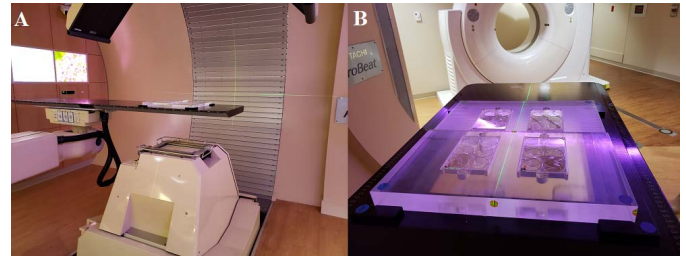
radiotherapy (eg, 6-MV x-rays) [17–20]. This enhancement may provide a small therapeutic advantage; however, finding methods for further increasing the therapeutic ratio for protons may offer additional benefits when treating traditionally radioresistant cancers.

Proton radiobiology is an active area of research, with additional work needed to continue to understand the underlying molecular and cellular mechanisms related to proton-induced cell death. Experiments in this area of research are time and resource intensive and are limited by beam availability because there are currently 35 operational proton centers in the US, as of January 2020, according to the Particle Therapy Co-Operative Group [21]. Therefore, the purpose of this study was to increase productivity in proton radiobiology–related research and maintain excellent dosimetric accuracy. This work introduces the design of a platform created for simultaneous irradiation of 4 cell culture plates with a spot-scanning proton beam.

Materials and Methods

Phantom Setup

This in vitro proton therapy research platform was created with the intention of mimicking patient treatment workflows for localization and delivery. Each treatment room in the proton therapy center (Pro Beat V, Hitachi, Japan) has a robotic couch system, able to localize patients within approximately 1 mm of accuracy. A couch top that docks with the robotic system was modified by cutting a hole through the center to allow for irradiation with a posterior beam (**Figure 1A**).

A computerized numeric-controlled milling machine was used to create an acrylic phantom, able to hold four 6-well cell culture plates (12.8 cm by 8.6 cm). The phantom was fitted over top of the couch cutout and indexed to ensure setup reproducibility. Cell culture plates were set down into the acrylic phantom such that the top of the phantom and the plate tops were flush (**Figure 1B**). Plates were positioned such that cells were located at the low-LET entrance (ENT) and at the high-LET Bragg peak (BP) portions of the BC. The amount of acrylic underneath the plate was varied to change the water-equivalent thickness (WET) and, therefore, the position of the cells along the BC.

To verify that the acrylic phantom was properly constructed and to demonstrate the accuracy of the WET, dual-ring multilayer ionization chamber (Hitachi Ltd, Hitachi Works, Hitachi, Japan) measurements were performed [22]. Physical measurements with calipers of both the bottoms of the 6-well plates and the acrylic phantoms were also taken to maintain submillimeter precision. Both sets of measurements allowed for the accurate calculation of the relative stopping power (RSP) of the material along the beam path to the location of the adherent cells. The RSP values (cast acrylic, $RSP = 1.16$) were then accounted for in the treatment-planning system for increased accuracy in the dose calculation of the experimental setup.

Treatment Planning

A treatment plan was created with the clinical treatment-planning system Eclipse (Varian Medical Systems, Palo Alto, California). A 76.8-MeV monoenergetic spot-scanning proton beam was used to create a uniform field encompassing all 4 cell culture plates in the acrylic phantom (**Figure 2A**). A mini pyramid filter (mPF) [23] was used to broaden the BP in the direction of the beam to a full-width half maximum of 7 mm (**Figure 2C**), for more-robust delivery. A 25-mm range shifter was also placed in the nozzle to shift the BP proximally to limit the amount of acrylic needed underneath the cell plates. The range of the resulting BP was 44.4 mm. A posterior beam arrangement was chosen to limit the air gap between the phantom and the plate holding the cells. With this arrangement, the air gap was limited to the lateral edges of the wells within the cell plates, which would have little dosimetric effect.

To ensure the same physical dose was delivered uniformly across all 4 plates, the spot weighting or monitor unit (MU) per spot was changed based on the difference in dose from the depth-dose profile for the 2 depths that the cells were placed at.

Figure 2. Treatment planning. (A) Monte Carlo dose for proton delivery, where red is the prescription dose, covering the plate bottom. (B) Dose-averaged linear energy transfer (LET) distribution covering the plate bottom, where blue is 1 keV/μm, and red is 10 keV/μm. (C) Dose (blue) and LET (red) profiles relative to depth for the 76.8-MeV proton beam with a mini pyramid filter and 25-mm range shifter. Circles denote the positions cells are placed along the Bragg curve in the experimental setup.
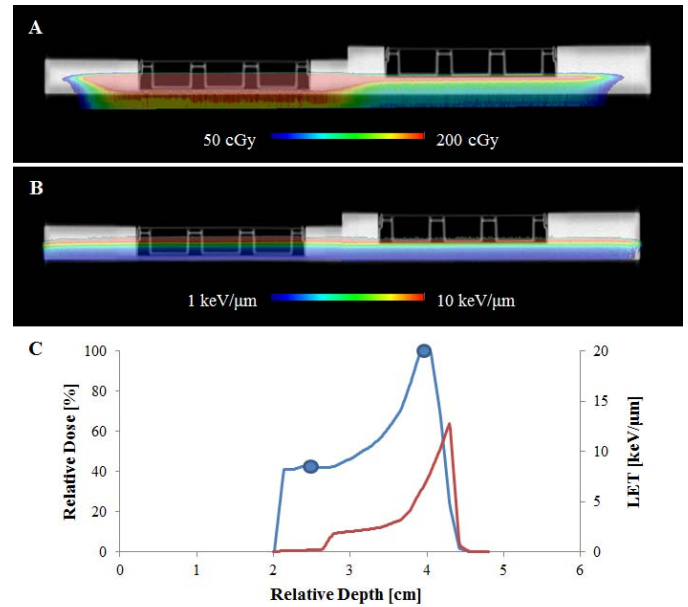
For example, the MU per spot delivered to cells positioned at the BP was 0.165 relative to the 0.327 MU/spot for the cells at the ENT position. To treat with a range of physical doses, the original plan was copied, and total MU was scaled appropriately.

Treatment plans created for in vitro proton irradiation were run in clinical mode, closely mimicking patient treatment workflows for setup and delivery. Each physical dose point was programmed as a separate treatment plan. The total time for treatment field delivery was roughly 4.5 min/1 Gy.

Dosimetric Verification

Dosimetric measurements were repeated 3 times with a Markus (PTW, Freiburg, Germany) parallel-plate chamber, placed in the corner closest to isocenter or at the edge of the radiation field in each of the plate inserts but without cell culture plates. The cap of the Markus chamber and the bottom of a cell culture plate are similar in WET; therefore, the sensitive volume of the chamber was at the same plane as the cells. The EBT3 radiochromic film (RCF; Ashland, Bridgewater, New Jersey, USA) was employed for secondary physical-dose measurements to compare with those of the Markus chamber and to measure the dose uncertainty across a single well. Film was cut and placed in the bottom of each well of the 4-cell culture plates positioned in the acrylic phantom. No water or medium was placed into the wells with the film because previous experience showed no dosimetric difference in measurements with or without 2 mL of water. Three measurements were made for each position (edge or center of the proton field) in all cell culture plates. Because RCF is known to underrespond in proton radiation fields, a correction was applied to the film readings for absolute dose measurements based on previous work [24]:

$U = -0.0251 \times LET_d + 1.02$. Measured dose from the film was divided by the correction factor U to obtain the final absolute dose. Dose uncertainty measured related to the film does not take LET_d uncertainty into account but is, rather, a measurement of variation in film response for a fixed LET_d value. Average LET_d values for a given depth of treatment were obtained from our in-house graphics processing unit–based Monte Carlo (MC) [25] and have been shown to match dose-averaged lineal energy measurements taken previously [26]. The MC simulated both the geometry and the material composition of all components in the beam path proximal to the cells, including the mPF, range shifter, and acrylic phantom. Both MC dose (MCD) and LET_d values were calculated for the 2 positions along the BC, and uncertainty was accounted for by quantifying the change in dose or LET_d, given a change in depth of ± 0.5 mm. A 2-dimensional colorwash image shows the distribution of the MCD (**Figure 2A**) and LET_d (**Figure 2B**) on a computed tomography scan of the phantom setup.

Biologic Verification

Clonogenic cell-survival assays were conducted with Chinese hamster ovary (CHO) cells (ATCC, Manassas, Virginia) as a final validation of the in vitro proton-irradiation setup proposed in this study. Detailed cell culture conditions have been published previously [27] but are briefly described. Cells were plated in triplicate wells 4 hours before irradiation in

Table 1. Dosimetric results. Monte Carlo dose and linear energy transfer (LET$_d$) calculations (mean $\pm$ 0.5 mm). Markus chamber and radiochromic film (RCF) measurements (mean $\pm$ 1 SD).

Bragg curve position	Position in the irradiation field	Markus physical dose (cGy)	Monte Carlo physical dose (cGy)	LET$_d$ corrected RCF dose (cGy)	LET$_d$ (keV/μm)
BP	Edge	202.8 ($\pm$ 0.3)	204.4 ($\pm$ 2.8)	212.3 ($\pm$ 1.4)	7.3 ($\pm$ 0.7)
BP	Center	209.8 ($\pm$ 0.1)	202.6 ($\pm$ 4.0)	218.7 ($\pm$ 1.1)	7.3 ($\pm$ 0.7)
BP	Average	206.3 ($\pm$ 3.8)	203.7 ($\pm$ 3.4)	215.5 ($\pm$ 3.6)	7.3 ($\pm$ 0.7)
ENT	Edge	190.1 ($\pm$ 0.5)	198.2 ($\pm$ 5.1)	195.3 ($\pm$ 1.8)	2.2 ($\pm$ 0.1)
ENT	Center	191.5 ($\pm$ 0.5)	196.8 ($\pm$ 4.7)	194.7 ($\pm$ 1.6)	2.2 ($\pm$ 0.1)
ENT	Average	190.8 ($\pm$ 0.8)	197.0 ($\pm$ 4.7)	195.0 ($\pm$ 1.6)	2.2 ($\pm$ 0.1)

Abbreviations: cGy, centigray; BP, Bragg peak; ENT, entrance.

concentrations ranging from 100 to 2000 cells/well depending on the delivered dose. The CHO cells were originally plated in 2 mL of medium before treatment. All cell culture plates were removed from the incubator for treatment and kept at room temperature for no longer than 1 hour. An additional 2 mL of medium was added 24 hours after exposure, and then, the cells were allowed to incubate for 1 week after treatment before the staining and analysis took place. Three independent runs were conducted for each dose point (0, 1, 2, 4, 6, and 8 Gy) and for each experiment (ENT and BP). Plated CHO cells were placed in each of the 4 inserts of the acrylic phantom. Analysis for cell survival was completed with the linear quadratic model, and error was propagated in the same way as demonstrated previously [27].

To assess the accuracy of the setup, clonogenic cell-survival assay results were compared with previously published work that used a single-plate setup and CHO cells at similar proton energies [28].

Results

Dosimetric Evaluation

The average measured doses from the Markus chamber and the RCF agreed to within 1.9% for the cell culture plates located in the ENT of the 76.8-MeV beam. Similarly, both measured doses for the plates located at the BP were closely matched to within 4.5%. The average measured doses from the Markus chamber and the MCD agreed to within 3.2% for the ENT and 1.3% for the BP plates. The largest discrepancy across the 2-dose measurements and 1-dose calculations was between the RCF and MCD data at the BP position where dosimetry differed on average by 5.8%. Dose across each plate, from the edge to the center, varied at most by 0.7% and 3.3% for ENT and BP plates, respectively. Dose across a single well was found to be fairly uniform with the average difference being $\pm$ 1.6%, and the maximum difference was $\pm$ 2.2%. **Table 1** summarizes the dosimetric results. Overall, positional uncertainty of the experimental setup is on the order of 1 mm, largely driven by the accuracy of the robotic arm in positioning the couch.

Biologic Verification

Survival curves for the CHO cells positioned at ENT and BP positions in the setup are shown in **Figure 3**. Fit parameters from the linear quadratic model are listed in **Table 2**. Increased cell death is shown in cells at the BP compared with the ENT, as expected. When comparing cell-survival data to previously published results under comparable experimental conditions, similar trends are seen between the 2 data sets. Survival curves from CHO cells irradiated with a lower energy of 71 MeV (LET$_d$ BP, 4.4 keV/μm; ENT, 1.8 keV/μm) showed increased cell death relative to the 76.8 MeV, as expected.

Discussion

Because of the large time commitment and resource requirements needed to conduct these in vitro experiments, a precise, high-throughput system has been built for cell-based proton radiobiology. Cell work often requires repeat, identical measurements. Treating individual plates separately is time consuming and increases the risk of introducing additional errors in the setup and timing of the experiment. Therefore, the platform developed in this study was focused on providing an accurate, high-throughput method for irradiating multiple in vitro experiments at once. Increased productivity in in vitro proton experimentation will be useful for studies such as evaluating varying biologic response to proton radiation in cells with genetic alterations or in combination with other therapeutic drugs.

Figure 3. Comparison of survival curves for Chinese hamster ovary cells irradiated with 6-MV x-rays [28] and 71- [28] or 76.8-MeV protons. Circles (open, data previously published; closed, data generated in this study) denote the mean survival (n = 3) at each dose point, and error bars indicate 1 SD. Dosimetric uncertainty is ± 1.9% for all points.
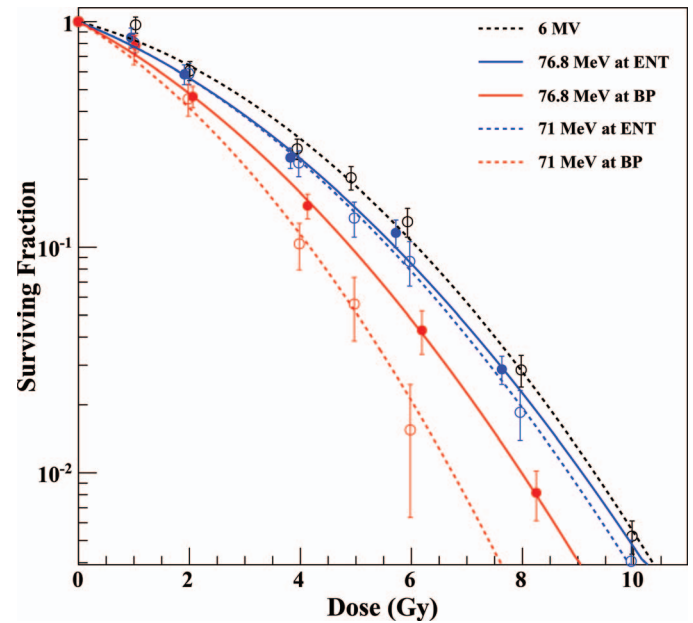
The setup facilitates simultaneous irradiation of 4 (6-well) cell culture plates, located at 2 points (ENT and BP) along the BC of a 76.8-MeV beam. Delivery of 1 Gy takes roughly 4.5 minutes using the proposed workflow. Although a single-plate workflow uses roughly the same amount of beam on time, the additional time needed between beams for setup decreases the overall efficiency. Further, our system has the potential to decrease overall human error by limiting the need to change the setup to change the depth at which the cells are positioned.

Dosimetric accuracy is important in radiobiologic experiments in which differences of biologic effects can be on the order of 10%. To make meaningful conclusions from these studies, associated uncertainties must be minimized. To quantify the dosimetric uncertainty of the in vitro proton irradiation platform, Markus chamber measurements, serving as the gold standard, were taken at various positions along the platform. A redundant physical measurement was made with an LET_d-corrected RCF to confirm our uncertainty and ensure the high standard for dosimetric accuracy was met. A third check on dosimetric accuracy was performed through the MC simulation, which also calculated the LET_d. These 3 methods for verifying the dosimetry of the setup provided additional confidence in the overall accuracy of the radiobiologic measurements that use this method.

Dosimetric uncertainties across the setup were within ± 1.8% of the mean dose on average, as measured with the Markus chamber. Uncertainty in dose across each plate was found to be larger for plates located at the BP relative to the ENT position. This may be due to the increase in beam divergence as the scanning beam moves further from isocenter. Because of that divergence, the proton path length differs depending on the location within the treatment field, where a greater deviation from isocenter results in an increase in path length. Therefore, beam divergence directly affects the delivered dose because the treatment plan is optimized to deliver the intended dose at a specific point of the central axis where there is no divergence. That has negligible effect on the dose delivered in the ENT region because the BC is relatively flat in that region and robust to

Table 2. Biologic verification of the experimental setup using Chinese hamster ovary cells. Fit parameters for the linear quadratic model (± 1 SD) were used to generate cell survival curves. Relative biologic effectiveness (RBE) values at 50% and 10% survival with errors are as reported in Howard et al [27] and Howard et al [28].

Energy and radiation type	Position along Bragg curve	α (Gy^{-1})	β (Gy^{-2})	RBE$_{50\%}$	RBE$_{10\%}$
6-MV x-rays[a]	—	0.15 (± 0.03)	0.04 (± 0.00)	1.00	1.00
71.3-MeV protons[a]	ENT	0.22 (± 0.04)	0.03 (± 0.01)	1.19 (± 0.10)	1.09 (± 0.04)
71.3-MeV protons[a]	BP	0.34 (± 0.10)	0.05 (± 0.02)	1.67 (± 0.23)	1.46 (± 0.08)
76.8-MeV protons	ENT	0.22 (± 0.04)	0.03 (± 0.00)	1.13 (± 0.09)	1.02 (± 0.01)
76.8-MeV protons	BP	0.31 (± 0.05)	0.04 (± 0.01)	1.48 (± 0.14)	1.28 (± 0.04)

Abbreviations: ENT, entrance; BP, Bragg peak.
[a]Data reproduced from references [27-28].

changes in path length. The differences in proton path length do have an effect on the absolute physical dose at the BP because both the LET and the dose change rapidly in that region. However, at positions within the cell culture plates in which the proton path length is increased, the deposited dose decreases as the LET increases, resulting in relatively small dosimetric differences. Variable LET was not accounted for in our film measurements across the BP plates because the film results agreed well with the Markus chamber measurements, which are independent of LET. Further, the dosimetric uncertainty was less than ± 2.5%, independent of the dose-quantification method used, which is reasonable for radiobiologic experiments, which generally aim for ± 5%. Finally, although there are small variabilities in both dose and LET across the radiation field because of the beam divergence, those uncertainties result in minimal effect on radiobiologic endpoints such as the RBE.

To verify that our dosimetric measurements corresponded to biologic differences, clonogenic cell survival assays were conducted with CHO cells. Survival curves showed decreased survival for cells placed at the BP, as expected [17, 18, 28–33] where increased depth and the slowing down of protons corresponds to increased cell death. Our previously published data set of CHO cell survival from a 71-MeV proton beam was used for comparison [28]. A higher-energy proton beam was chosen for this setup to ensure a dosimetrically robust delivery. Lower proton energies have narrower BPs and thus a smaller full-width half maximum relative to higher energies. Because of the divergence of the beam at locations furthest from isocenter, a wider beam was needed to maintain dosimetric accuracy for all plates within the radiation field. Cell death in plates irradiated with 71-MeV protons was more pronounced relative to the cells irradiated in this study with a 76.8-MeV beam and can be seen in the higher-RBE values in **Table 2**. Although direct comparisons of biologic data sets measuring proton RBE are difficult because of the numerous dependencies (eg, cell type, proton energy, and modulation of the proton beam; biological endpoint; reference radiation; and LET), our data agreed well with previously published data [16, 28]. A study by Marshall and colleagues [34] measured similar proton RBE at 50% survival values in human fibroblast cells ranging from 1.03 (± 0.68) to 1.72 (± 1.14) with LET_d values ranging from 0.63 keV/μm in the ENT to 7.5 keV/μm on the distal edge of a 219.65-MeV spread-out BP [34]. Britten et al [2] studied a similar cell line, the V79 Chinese hamster fibroblast line, measuring proton RBE at 10% survival values ranging from 1.23 to 1.78 along a modulated 87-MeV spread-out BP.

Other efforts have been made to increase the efficiency of in vitro–based proton radiobiology research. Guan et al [29] proposed a sophisticated setup for 96-well plates with varying thicknesses of the jig holding the cells to alter the position of the cells on the BC. Although their setup allowed for multiple measurement points along the BC, it also included additional film on top of the jig for accurate positioning along the distal falloff region. Our proposed setup, although simpler, avoids a complex configuration and, therefore, decreases the potential to introduce additional setup errors. This work aimed to expand upon previous studies by both measuring and simulating the dosimetry and thereby increasing the confidence in reported dosimetric uncertainty.

Proton radiobiology remains an active area of research, with in vitro studies having a fundamental role. Continued efforts to understand the intricacies of the biologic effect of proton therapy will aid in more-tailored, patient-specific approaches to radiation treatments in the future. The platform presented in this work allows for an increase in productivity for in vitro studies and maintains a high level of dosimetric accuracy.

ADDITIONAL INFORMATION AND DECLARATIONS

References

1. Held KD, Kawamura H, Kaminuma T, Paz AES, Yoshida Y, Liu Q, Willers H, Takahashi A. Effects of charged particles on human tumor cells. *Front Oncol*. 2016;6:23.

2. Britten RA, Nazaryan V, Davis LK, Klein SB, Nichiporov D, Mendonca MS, Wolanski M, Nie X, George J, Keppel C. Variations in the RBE for cell killing along the depth-dose profile of a modulated proton therapy beam. *Radiat Res*. 2013; 179:21–8.

3. Matsumoto Y, Matsuura T, Wada M, Egashira Y, Nishio T, Furusawa Y. Enhanced radiobiological effects at the distal end of a clinical proton beam: in vitro study. *J Radiat Res*. 2014;55:816–22.

4. Belli M, Cherubini R, Finotto S, Moschini G, Sapora O, Simone G, Tabocchini MA. RBE-LET relationship for the survival of V79 cells irradiated with low energy protons. *Int J Radiat Biol*. 1989;55:93–104.

5. Belli M, Bettega D, Calzolari P, Cera F, Cherubini R, Dalla Vecchia M, Durante M, Favaretto S, Gialanella G, Grossi G, Marchesini R, Moschini G, Piazzola A, Poli G, Pugliese M, Sapora O, Scampoli P, Simone G, Sorrentino E, Tabocchini MA, Tallone L, Tiveron P. Inactivation of human normal and tumour cells irradiated with low energy protons. *Int J Radiat Biol*. 2000;76:831–9.

6. Gueulette J, Gregoire V, Octave-Prignot M, Wambersie A. Measurements of radiobiological effectiveness in the 85 MeV proton beam produced at the cyclotron CYCLONE of Louvain-la-Neuve, Belgium. *Radiat Res*. 1996;145:70–4.

7. Kim SS, Choo DW, Shin D, Baek HJ, Kim TH, Motoyama N, De Coster BM, Gueulette J, Furusawa Y, Ando K, Cho KH. In vivo radiobiological characterization of proton beam at the National Cancer Center in Korea: effect of the *Chk2* mutation. *Int J Radiat Oncol*. 2011;79:559–62.

8. Chaudhary P, Marshall TI, Perozziello FM, Manti L, Currell FJ, Hanton F, McMahon SJ, Kavanagh JN, Cirrone GAP, Romano F, Prise KM, Schettino G. Relative biological effectiveness variation along monoenergetic and modulated Bragg peaks of a 62-MeV therapeutic proton beam: a preclinical assessment. *Int J Radiat Oncol Biol Phys*. 2014;90:27–35.

9. Sørensen BS, Overgaard J, Bassler N. In vitro RBE-LET dependence for multiple particle types. *Acta Oncol*. 2011;50:757–62.

10. Gerelchuluun A, Hong Z, Sun L, Suzuki K, Terunuma T, Yasuoka K, Sakae T, Moritake T, Tsuboi T. Induction of in situ DNA double-strand breaks and apoptosis by 200 MeV protons and 10 MV X-rays in human tumour cell lines. *Int J Radiat Biol*. 2011;87:57–70.

11. Aoki-nakano M, Furusawa Y, Uzawa A, Matsumoto Y, Hirayama R, Tsuruoka C, Ogino T, Nishio T, Kagawa K, Murakami M, Kagiya G, Kume K, Hatashita M, Fukuda S, Yamamoto K, Fuji H, Murayama S, Hata M, Sakae T, Matsumoto H. Relative biological effectiveness of therapeutic proton beams for HSG cells at Japanese proton therapy facilities. *J Radiat Res*. 2014;55:812–5.

12. Ando K, Furusawa Y, Suzuki M, Nojima K, Majima H, Koike S, Aoki M, Shimizu W, Futami Y, Ogino T. Relative biological effectiveness of the 235 MeV proton beams at the National Cancer Center Hospital East. *J Radiat Res*. 2001;42:79–89.

13. Calugaru V, Nauraye C, Noël G, Giocanti N, Favaudon V, Mégnin-Chanet F. Radiobiological characterization of 2 therapeutic proton beams with different initial energy spectra used at the Institut Curie Proton Therapy Center in Orsay. *Int J Radiat Oncol Biol Phys*. 2011;81:1136–43.

14. Inada T, Kawachi K, Kanai T, Nojiri I. Inactivation of cultured human tumor cells irradiated by cyclotron neutrons and protons. *J Radiat Res*. 1981;22:143–53.

15. Maeda K, Yasui H, Matsuura T, Yamamori T, Suzuki M, Nagane M, Nam JM, Inanami O, Shirato H. Evaluation of the relative biological effectiveness of spot-scanning proton irradiation in vitro. *J Radiat Res*. 2016;57:307–11.

16. Paganetti H. Relative biological effectiveness (RBE) values for proton beam therapy: variations as a function of biological endpoint, dose, and linear energy transfer. *Phys Med Biol*. 2014;59:R419–72.

17. Paganetti H, Niemierko A, Ancukiewicz M, Gerweck LE, Goitein M, Loeffler JS, Suit HD. Relative biological effectiveness (RBE) values for proton beam therapy. *Int J Radiat Oncol Biol Phys*. 2002;53:407–21.

18. Paganetti H. Proton Relative Biological Effectiveness - Uncertainties and Opportunities. *Int J Part Ther*. 2018;5:2–14.

19. Paganetti H, Blakely E, Carabe-fernandez A, Carlson DJ, Held KD. Report of the AAPM TG-256 on the relative biological effectiveness of proton beams in radiation therapy. *Med Phys*. 2019;46:e53–78.

20. Michaelidesová A, Vachelová J, Puchalska M, Brabcová KP, Vondráček V, Sihver L, Davídková M. Relative biological effectiveness in a proton spread-out Bragg peak formed by pencil beam scanning mode. *Australas Phys Eng Sci Med*. 2017;40:359–68.

21. [PTCOG] Particle Therapy Co-Operative Group. Facilities in operation. https://www.ptcog.ch/index.php/facilities-in-operation. Published 2015. Accessed February 5, 2020.

22. Takayanagi T, Nihongi H, Nishiuchi H, Tadokoro M, Ito Y, Nakashima C, Fujitaka S, Umezawa M, Matsuda K, Sakae T, Terunuma T. Dual ring multilayer ionization chamber and theory-based correction technique for scanning proton therapy. *Med Phys*. 2016;43:4150–62.

23. Remmes N, Courneyea L, Corner S, Beltran C, Stoker J, Kemp B, Kruse J, Herman M. WE-F-16A-02: design, fabrication, and validation of a 3D-printed proton filter for range spreading. *Med Phys*. 2014;41:514.

24. Anderson SE, Grams MP, Wan Chan Tseung H, Furutani KM, Beltran CJ. A linear relationship for the LET-dependence of Gafchromic EBT3 film in spot-scanning proton therapy. *Phys Med Biol*. 2019;64:055015.

25. Wan Chan Tseung HS, Ma J, Beltran C. A fast GPU-based Monte Carlo simulation of proton transport with detailed modeling of nonelastic interactions. *Med Phys*. 2015;42:2967–78.

26. Anderson SE, Furutani KM, Tran LT, Chartier L, Petasecca M, Lerch M, Prokopovich DA, Reinhard M, Perevertaylo VL, Rosenfeld AB, Herman MG, Beltran C. Microdosimetric measurements of a clinical proton beam with micrometer- sized solid-state detector. *Med Phys*. 2017;44:6029–37.

27. Howard M, Beltran C, Sarkaria J, Herman MG. Characterization of relative biological effectiveness for conventional radiation therapy: a comparison of clinical 6 MV x-rays and [137]Cs. *J Radiat Res*. 2017;58:608–613.

28. Howard ME, Beltran C, Anderson S, Tseung WC, Sarkaria JN, Herman MG. Investigating dependencies of relative biological effectiveness for proton therapy in cancer cells. *Int J Part Ther*. 2017;4:12–22.

29. Guan F, Bronk L, Titt U, Lin SH, Mirkovic D, Kerr MD, Zhu XR, Dinh J, Sobieski M, Stephan C, Peeler CR, Taleei R, Mohan R, Grosshans DR. Spatial mapping of the biologic effectiveness of scanned particle beams: towards biologically optimized particle therapy. *Sci Rep*. 2015;5:9850.

30. Wouters BG, Lam GK, Oelfke U, Gardey K, Durand RE, Skarsgard LD. Measurements of relative biological effectiveness of the 70 MeV proton beam at TRIUMF using Chinese hamster V79 cells and the high-precision cell sorter assay. *Radiat Res*. 1996;146:159–70.

31. Courdi A, Brassart N, Hérault J, Chauvel P. The depth-dependent radiation response of human melanoma cells exposed to 65 MeV protons. *Br J Radiol*. 1994;67:800–4.

32. Petrović I, Ristić-Fira A, Todorović D, Korićanac L, Valastro L, Cirrone P, Cuttone G. Response of a radioresistant human melanoma cell line along the proton spread-out Bragg peak. *Int J Radiat Biol*. 2010;86:742–51.

33. Cuaron JJ, Chang C, Lovelock M, Higginson DS, Mah D, Cahlon O, Powell S. Exponential increase in relative biological effectiveness along distal edge of a proton Bragg peak as measured by deoxyribonucleic acid double-strand breaks. *Int J Radiat Oncol Biol Phys*. 2016;95:62–9.

34. Marshall TI, Chaudhary P, Michaelidesová A, Vachelová J, Davídková M, Vondráček V, Schettino G, Prise KM. Investigating the implications of a variable RBE on proton dose fractionation across a clinical pencil beam scanned spread-out Bragg peak. *Int J Radiat Oncol Biol Phys*. 2016;95:70–7.